

Giant resonant enhancement of the nonstationary holographic currents in an alternating electric field

Mikhail Bryushinin,* Vladimir Kulikov, and Igor Sokolov
A.F. Ioffe Physical Technical Institute, 194021, St. Petersburg, Russia
 (Received 9 September 2002; published 7 February 2003)

We report the resonant excitation of the nonstationary holographic currents in photoconductive crystals placed in a sinusoidal electric field. The analysis of the effect is performed for the simplest model of a semiconductor with monopolar photoconductivity. We demonstrate that the frequency transfer function of the effect has a maximum at $\omega_r \approx K\mu E_0$ originating from the resonant excitation of photoconductivity gratings. The dependences of the holographic current amplitude versus effective value of the ac electric field E_0 , spatial frequency of the interference pattern K , and light intensity I_0 are measured in the photorefractive n -type $\text{Bi}_{12}\text{SiO}_{20}$ crystal. The drift mobility of electrons is estimated from the position of the resonant peak on the frequency transfer function of the effect: $\mu = 0.13\text{--}0.8 \text{ cm}^2/\text{V s}$. The advantages of the photocurrent generation in ac fields are pointed out, and possible practical applications of the effect are discussed.

DOI: 10.1103/PhysRevB.67.075202

PACS number(s): 72.20.Jv, 42.70.Nq

I. INTRODUCTION

During the last decades several methods increasing the efficiency of the holographic recording in photorefractive materials were developed. Most of them combine the nonstationary recording and application of an external electric field to the crystal.¹ Two basic ways to increase the space charge field grating amplitude are usually distinguished: the former method includes the application of a dc external electric field to the sample illuminated by a running interference pattern,² and the latter one implies the application of an ac field along with a stationary interference pattern.³ The physical principles of these techniques are different: the former method is resonant and based on the synchronization of the interference pattern with a fundamental space charge wave; the latter one is nonresonant and based on the enhanced symmetric redistribution of charge carriers between bright and dark fringes similar to the diffusion regime of grating formation. A number of relative techniques using combinations of moving or oscillating light pattern and dc and ac electric fields have been carried out in photorefractive materials.^{4–8}

The nonstationary holographic photocurrent⁹ [or non-steady-state photo-emf (Ref. 10)] is a holography-related effect observed in wide-gap crystals. It appears in a semiconductor material illuminated by an oscillating light pattern. Such illumination is usually created by two coherent light beams, one of which is phase modulated with frequency ω . The alternating current results from the periodic relative shifts of the photoconductivity and space charge gratings which arise in the crystal's volume under illumination. Like the holographic recording in photorefractive crystals this effect demonstrates adaptive properties that promote its application in such areas as vibration monitoring, velocimetry, etc.¹¹ In contrast to the holographic methods this technique allows the direct transformation of phase-modulated optical signals into the electrical current and can be applied for the characterization of centrosymmetrical and even amorphous materials. Since the photocurrent originates from the interaction of both the photoconductivity and space charge gratings,

a lot of photoelectric parameters can be measured: Maxwell relaxation time τ_M and average photoconductivity σ_0 , carrier's lifetime τ and mobility μ , diffusion L_D and drift L_0 lengths, Debye screening length l_D , and concentration of trapping centers N_D^+ .¹⁰

The excitation of the nonstationary photocurrents in an external electric field significantly differs from the diffusion regime. When a strong dc voltage is applied to the crystal two resonant peaks can be observed on the frequency transfer function of the effect. The first one is associated with resonant excitation of the space charge gratings.^{12,13} The second maximum appears when the velocities of the interference pattern and photocarriers drifting in the electric field are equal.^{12,14} The drift mobility can be easily estimated from the position of this resonant peak. So the photo-emf technique provides the possibility for an eigenwave investigation in semiconductors placed in an external electric field.

Earlier investigations of photocurrent excitation in an alternating electric field have shown that application of a high-frequency electric field results in the nonresonant enhancement of the signal amplitude.^{15,16} This effect was observed for low frequencies of phase modulation ($\omega < \Omega$) where the influence of the electric field can be considered as "enhanced diffusion" of carriers recording the space charge distribution with large amplitude. For this reason the frequency transfer function of the effect maintains a form typical for the diffusion regime: the linear growth of the signal for low frequencies of phase modulation following by a frequency-independent region.

Up to now no attempts to study the influence of an ac field on the nonstationary photocurrent excitation for high frequencies of phase modulation ($\omega > \Omega$, $\tau_M^{-1} < \Omega < \tau$) have been made. Meanwhile, such a combination of frequencies can give a unique opportunity for the signal magnification. Indeed the frequency of the external field is higher than the inverse formation time of the space charge grating with period $\Lambda = 2\pi/K$, $\Omega > |\tau_M(1 + K^2L_D^2 + iKL_0)|^{-1}$, so the space charge amplitude will be increased as was predicted in Ref. 3. At the same time the frequency of the external field is

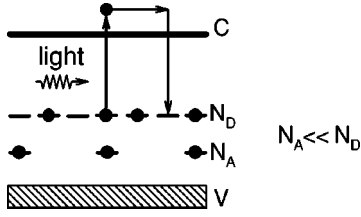


FIG. 1. Model of a semiconductor with one type of partially compensated donor centers and monopolar photoconductivity.

lower than the inverse relaxation time of the conductivity grating: $\Omega < |(1 + K^2 L_D^2 + i K L_0) \tau^{-1}|$. For this reason the amplitude of the photoconductivity grating will be increased as well via a resonant mechanism analogous to that discussed in Refs. 12 and 14. As a result the resonant signal enhancement in an ac electric field is expected to be more pronounced than for the case of the dc field.

In this paper we present experimental and theoretical results on the resonant excitation of nonstationary holographic currents in semiconductor crystals placed in a high-frequency electric field. In Sec. II we analyze theoretically the photocurrent generation in a sinusoidal electric field and describe the experimental setup, in Sec. III we present the results of the photocurrent measurements in *n*-type photorefractive $\text{Bi}_{12}\text{SiO}_{20}$, and in Sec. IV we discuss the possibilities and advantages of the proposed technique.

II. ANALYSIS OF THE EFFECT AND EXPERIMENTAL ARRANGEMENT

Let us suppose that the crystal is illuminated with the oscillating interference pattern formed by two plane light waves, one of which is phase modulated with frequency ω and amplitude Δ :

$$I(x, t) = I_0 [1 + m \cos(Kx + \Delta \cos \omega t)]. \quad (1)$$

Here I_0 is the average light intensity, m is the contrast, and K is the spatial frequency of the interference pattern. The sinusoidal electric field with amplitude E_{ext} and frequency Ω is applied to the crystal: $E_{ext}(t) = E_{ext} \cos \Omega t$. For the external field we use the effective value $E_0 = E_{ext} / \sqrt{2}$ rather than amplitude E_{ext} .

For the case of cyclic boundary conditions the total electric current averaged over the interelectrode spacing L contains the drift and displacement components. The non-steady-state photo-emf signal is defined by the drift one:¹⁰

$$j(t) = \frac{1}{L} \int_0^L e \mu n(x, t) E(x, t) dx. \quad (2)$$

Here e is the electron charge, $n(x, t)$ is the concentration of electrons in the conduction band, and $E(x, t)$ is the electric field.

In order to calculate distributions $n(x, t)$ and $E(x, t)$ we considered the widely used model of semiconductors with monopolar photoconductivity and one type of partially compensated donor levels (Fig. 1).^{1,17} The illumination leads to the generation of electrons from donor levels to the conduc-

tion band where they migrate due to the diffusion or drift mechanisms and recombine back to the donors. We studied the case of a “relaxation-type” semiconductor, i.e., $\tau \ll \tau_M$. The opposite situation (i.e., $\tau \gg \tau_M$) is slightly more complicated for the analysis, moreover the application of strong electric fields decreases the time constant of the conductivity relaxation and increases the buildup time for the space charge, so we obtain conditions analogous to the “relaxation-type” regime.

We suppose also that the frequency of the phase modulation ω is much higher than the frequency of the external electric field Ω ; the period of the ac field is larger than the carrier lifetime τ and shorter than the grating relaxation time τ_M :

$$\omega \gg \Omega, \quad (3)$$

$$\tau_M^{-1} \ll \Omega \ll \tau^{-1}. \quad (4)$$

The calculation procedure includes the solution of the balance, continuity, and Poisson equations. Since the main stages of this procedure are similar to the ones described in Ref. 16, we omit them and write the final expression for the complex amplitude of the photocurrent with frequency ω :

$$j^\omega = -\frac{m^2 \Delta}{2} \sigma_0 \left(E_D + E_0 \frac{K L_0}{1 + K^2 L_D^2} \right) \times \frac{1 + K^2 L_D^2 + i \omega \tau}{(1 + K^2 L_D^2 + i \omega \tau)^2 + K^2 L_0^2}. \quad (5)$$

Here $E_D = (k_B T / e) K$ is the diffusion field and $L_0 = \mu \tau E_0$ is the drift length of photocarriers, k_B is the Boltzmann constant, and T is the temperature.

The resonant maximum appears in the frequency transfer function of the photocurrent when the drift item in this expression dominates over the diffusion one: $E_0 \gg E_D$, $K L_0 \gg 1 + K^2 L_D^2$. Then the resonant frequency and corresponding signal amplitude are equal to

$$\omega_r = \frac{K L_0}{\tau} = K \mu E_0, \quad (6)$$

$$j^\omega(\omega_r) = -\frac{m^2 \Delta \sigma_0 E_0 K L_0}{4(1 + K^2 L_D^2)^2}. \quad (7)$$

Let us compare the photocurrent excitation in the dc and ac fields for the considered frequency region: $\omega \gg \tau_M^{-1}$. The photocurrent amplitude in dc electric field was found to be¹²⁻¹⁴

$$j_{dc}^\omega = \frac{m^2 \Delta}{2} \sigma_0 \frac{E_0 K L_0 - E_D (1 + K^2 L_D^2 + i \omega \tau)}{(1 + K^2 L_D^2 + i \omega \tau)^2 + K^2 L_0^2}. \quad (8)$$

As seen the frequency transfer functions of the photocurrent for ac and dc fields are similar: the resonant peaks appear at the same frequency [Eq. (6)]. However there are distinctive

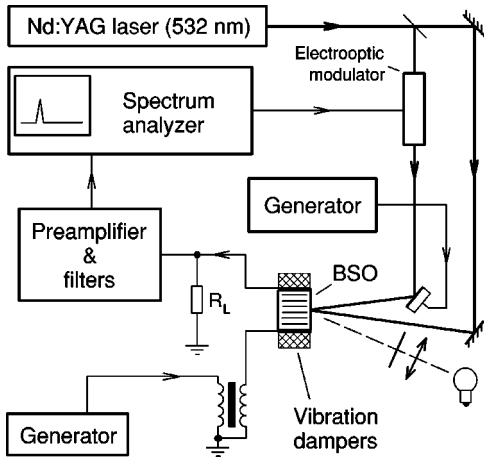


FIG. 2. Experimental setup for measurements of the non-steady-state photo-emf in an alternating electric field.

features which differ in these approaches. The resonant amplitude of the photocurrent excited in dc field equals

$$j_{dc}^{\omega}(\omega_r) = -i \frac{m^2 \Delta \sigma_0 E_0}{4(1 + K^2 L_D^2)}. \quad (9)$$

It is $KL_0/(1 + K^2 L_D^2)$ times lower than those for ac field [Eq. (7)]. Moreover, this difference grows when the amplitude of the applied field increases. Such an advantage of the ac voltage over the dc one is associated with the fact that the ac field enhances the stationary space charge grating proportionally to $\propto E_0^2$ (while the dc field does $\propto E_0$).³

The phases of the photocurrent amplitude defined by Eqs. (7) and (9) differ by $\pi/2$, which is due to the fact that the spatial shift of the stationary electric field grating is equal to $-\pi$ for the dc field and $-\pi/2$ for the ac field applied.¹

Besides one can note the different shapes of the resonant peak for the cases of ac and dc external fields [compare Eqs. (5) and (8)].

Measurements of the nonstationary holographic currents under an applied alternating electric field were carried out using the experimental setup shown in Fig. 2. The second harmonic of a Nd:YAG laser ($\lambda = 532$ nm) with an average power of $P_{out} \approx 50$ mW was used as the basic source of coherent radiation. A conventional Twyman-Green interferometer forms the interference pattern with a specified fringe spacing. The contrast of the interference pattern was settled to be small enough ($m = 0.12$) to avoid excitation of the higher spatial harmonics of the electric field grating. An electro-optic phase modulator ML-102A produced phase modulation of the laser beam with frequency ω and amplitude $\Delta = 0.81$. The additional low-frequency phase modulation with frequency 100 Hz and amplitude 2.4 rad was utilized for the separation of the volume and contact signals.¹⁸ This technique allows us to transfer the contact component of the signal to the side frequencies which are rejected by the selective receiver. As a result the signal detected at carrier frequency contains the volume component only. The photocurrent signal arising in the crystal's volume was amplified, filtered, and then measured by spectrum analyzer SK4-58 ($f = 0.4$ –600 kHz, $\Delta f = 100$ Hz, with 10 Hz videofilter). In

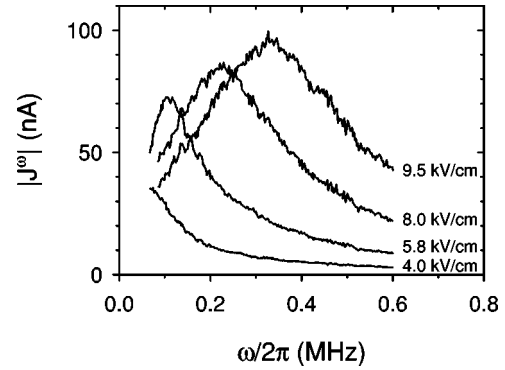


FIG. 3. Frequency transfer functions of the holographic current measured in photorefractive $\text{Bi}_{12}\text{SiO}_{20}$ for different effective values of the sinusoidal electric field: $E_0 = 4.0, 5.8, 8.0, 9.5$ kV/cm ($\lambda = 532$ nm, $I_0 = 2.2$ W/cm², $K = 500$ cm⁻¹, $\Omega/2\pi = 6$ kHz).

our experiments we used an *n*-type $\text{Bi}_{12}\text{SiO}_{20}$ crystal with characteristic dimensions $1 \times 4 \times 10$ mm³, the front and back surfaces of the crystal (1×10 mm²) were polished, and the silver paste electrodes (4×3 mm²) were painted on the lateral surfaces. The interelectrode spacing was $L = 1$ mm. The crystal was placed in the Teflon holder with Styrofoam linings which damp the mechanical oscillations due to the piezoelectric effect. The sinusoidal voltage from the generator ($\Omega/2\pi = 6$ kHz) was amplified by a conventional transformer and then applied to the sample. In some experiments the crystal was simultaneously illuminated by light from a microscope lamp focused by a lens and passed through different filters: IKS-5 ($\lambda_{IR} = 980$ –3000 nm) KS-15 ($\lambda_R = 650$ –2700 nm), and SZS-22 ($\lambda_B = 380$ –530 nm). The crystal's temperature was measured by the PtRh-Pt thermocouple.

III. EXPERIMENTAL RESULTS

Figure 3 presents the frequency transfer functions of the nonstationary holographic photocurrent measured for different amplitudes of the external electric field $E_0 = U_0/L$ (U_0 is the effective amplitude of the applied voltage). The resonant maximum appears in the investigated frequency region ($\omega/2\pi = 60$ –600 kHz) when the effective value of the sinusoidal field reaches ~ 5 kV/cm. The further increase of the applied voltage leads to a nonlinear growth of the resonant frequency and current amplitude (Figs. 3 and 4).

The photocurrent amplitude grows slower than E_0^2 , which is probably due to nonlinear effects. The stationary electric field grating has amplitude $\sim mE_0KL_0$.¹⁶ When this value approaches the amplitude of the external field $E_{ext} = \sqrt{2}E_0$ we can expect the saturation of the photocurrent. For the chosen m and K and for $\mu\tau \sim 10^{-6}$ cm²/V,^{13,16} the discussed effect should appear at $E_0 \sim 2$ kV/cm. A similar saturation of the photocurrent was observed and discussed in Ref. 13 where the amplitude of the moving grating increases up to the value of the applied dc field.

The nonlinear dependence $\omega_r(E_0)$ points to the fact that strong electric fields influence the electron mobility, varying in the range $\mu = 0.19$ –0.43 cm²/V s (Fig. 5). The depen-

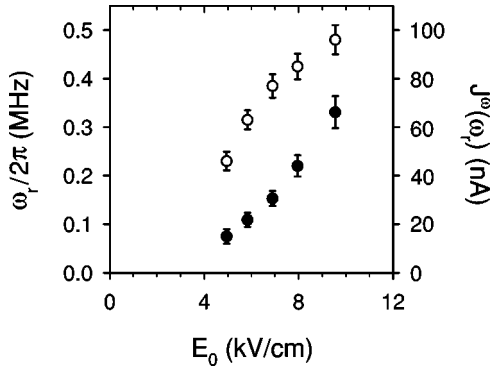


FIG. 4. The resonant frequency ω_r (●) and resonant photocurrent amplitude $J^\omega(\omega_r)$ (○) vs effective value of the external field E_0 ($\lambda=532$ nm, $I_0=2.2$ W/cm², $K=500$ cm⁻¹, $\Omega/2\pi=6$ kHz).

dependence $\mu(E_0)$ was approximated with the power function: $\mu \propto E_0^{1.3}$. Such behavior is most probably explained by heating of the sample in the electric field. Indeed, the crystal's temperature rises by ~ 20 K in an external field of 9.5 kV/cm (Fig. 5).

The forbidden gap of sillenite-type crystals is characterized by a rather complicated structure of the local levels.¹ In particular, the shallow traps affect the charge transport, significantly magnifying the conductivity relaxation time and reducing the effective drift mobility of electrons.¹⁷ When the temperature grows electrons spend less time being captured on shallow traps, so the effective mobility increases.

The dependences of the resonant frequency and photocurrent amplitude versus spatial frequency of the interference pattern are presented in Fig. 6. The dependence $\omega_r(K)$ is well fitted with the linear function as predicted by Eq. (6). This approximation allows us to estimate the electron mobility: $\mu=0.42$ cm²/V s ($T\approx 313$ K). This value is more than one order of magnitude higher than the ones measured earlier by the non-steady-state photocurrent technique in an external dc electric field.^{12,14} In contrast to the electric field the spatial frequency of the interference pattern does not influence the photoelectric parameters (lifetime, mobility, etc.), so the behavior of the resonant frequency is in good agreement with

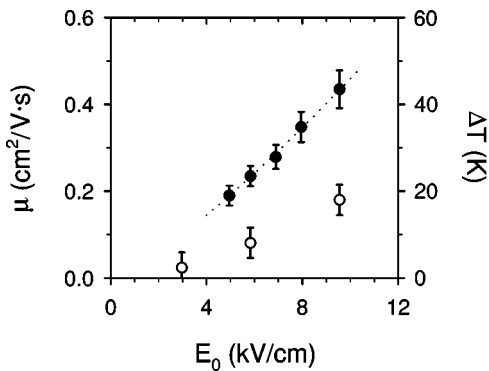


FIG. 5. Dependence of the drift mobility μ (●) vs effective value of the external field E_0 ($\lambda=532$ nm, $I_0=2.2$ W/cm², $K=500$ cm⁻¹, $\Omega/2\pi=6$ kHz). The dotted line shows fitting function $\mu \propto E_0^{1.3}$. The increment of the crystal's temperature $\Delta T=T-293$ K vs the external field amplitude E_0 is shown as well (○).

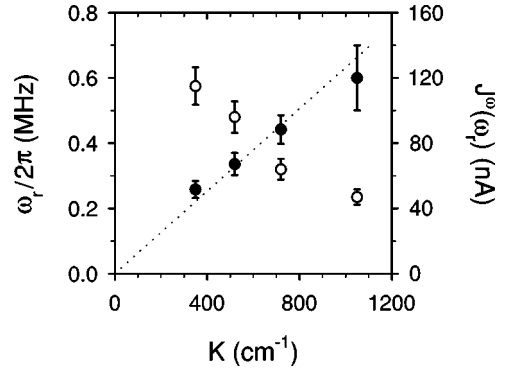


FIG. 6. Dependencies of the resonant frequency ω_r (●) and resonant photocurrent amplitude $J^\omega(\omega_r)$ (○) on the spatial frequency of the interference pattern K ($\lambda=532$ nm, $I_0=2.2$ W/cm², $E_0=9.5$ kV/cm, $\Omega/2\pi=6$ kHz, $T\approx 313$ K). The dotted line shows the approximation by Eq. (6) for $\mu=0.42$ cm²/V s.

the simplest theory presented in Sec. II, and we can state that the maximum on the frequency transfer functions of the photocurrent is associated with the resonant excitation of the photoconductivity gratings.

As seen from Fig. 6 the photocurrent amplitude is maximal for the lowest settled spatial frequency $K=3 \times 10^2$ cm⁻¹ though the theoretical estimation by Eq. (7) predicts a maximum at $K=(\sqrt{3}L_D)^{-1} \sim 6 \times 10^3$ cm⁻¹ ($L_D \sim 1$ μ m). Perhaps this discrepancy is typical for sillenites (compare with Ref. 13) and associated with the grating saturation effect discussed above.

The dependences of the resonant frequency and current amplitude versus light intensity are shown in Fig. 7. According to the basic theory presented above no dependence of the resonant frequency ω_r should be observed [Eq. (6)]. In practice, however, this statement is not valid since light intensity can influence the effective mobility (Fig. 8) via at least two mechanisms. First, the mobility increases due to Joule heat-

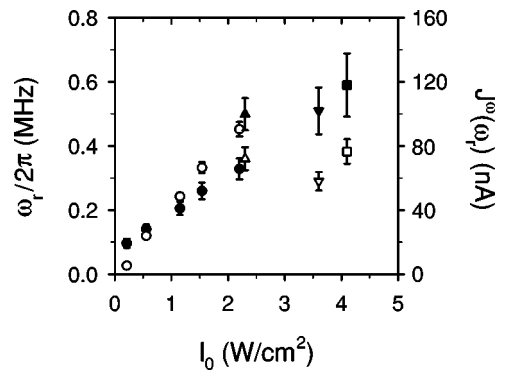


FIG. 7. The resonant frequency ω_r (●, ▲, ▼, ■) and resonant photocurrent amplitude $J^\omega(\omega_r)$ (○, △, ▽, □) vs total light intensity I_0 ($K=500$ cm⁻¹, $E_0=9.5$ kV/cm, $\Omega/2\pi=6$ kHz). The circles (●, ○) demonstrate the measurements with the only laser illumination ($\lambda=532$ nm); the other symbols correspond to the measurements with additional illumination: ▲, △: $\lambda_B=380-530$ nm, $I_B=0.10$ W/cm². ▼, ▽: $\lambda_{IR}=980-3000$ nm, $I_{IR}=1.4$ W/cm². ■, □: $\lambda_R=650-2700$ nm, $I_R=1.9$ W/cm².

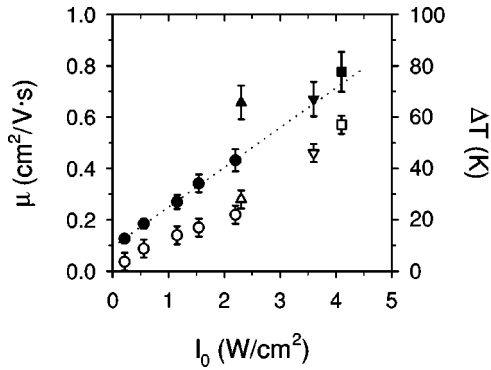


FIG. 8. Dependence of the drift mobility μ on the total light intensity I_0 ($K=500 \text{ cm}^{-1}$, $E_0=9.5 \text{ kV/cm}$, $\Omega/2\pi=6 \text{ kHz}$). Dependence $\mu(I_0)$ measured without additional illumination (\bullet) is fitted by the linear function $\mu \propto I_0$ with $\mu(0)=0.95 \text{ cm}^2/\text{V s}$. The other solid symbols present experiments with additional illumination: \blacktriangle : $\lambda_B=380\text{--}530 \text{ nm}$, $I_B=0.10 \text{ W/cm}^2$. \blacktriangledown : $\lambda_{IR}=980\text{--}3000 \text{ nm}$, $I_{IR}=1.4 \text{ W/cm}^2$. \blacksquare : $\lambda_R=650\text{--}2700 \text{ nm}$, $I_R=1.9 \text{ W/cm}^2$. The dependence of the temperature increment $\Delta T = T - 293 \text{ K}$ on the light intensity I_0 is shown by the corresponding open symbols.

ing of the illuminated crystal placed in the electric field. Second, the increase of the light intensity changes the population of the shallow traps; the capture rate of electrons to these traps becomes weaker, which consequently increases the effective mobility. As a result we obtained a wide range for electron mobility: $\mu=0.13\text{--}0.43 \text{ cm}^2/\text{V s}$. Similar behavior of the photocurrent was observed earlier for the case of dc external field.¹⁴

In order to vary the total light intensity and spectrum the crystal was illuminated by the additional infrared, red, blue, and “white” light from the microscope lamp (Figs. 7 and 8). The most powerful “white” light with intensity $I_W=2.9 \text{ W/cm}^2$ shifts the resonant maximum beyond the studied frequency range ($\omega_s/2\pi > 600 \text{ kHz}$), which correspond to the value of the drift mobility: $\mu > 0.8 \text{ cm}^2/\text{V s}$ ($T \approx 370 \text{ K}$).

The dependence of the resonant peak amplitude on the light intensity ($\lambda=532 \text{ nm}$) was found to be linear (Fig. 7), which is associated with the linear character of the photoconductivity. As seen from the same figure the additional illumination suppresses the signal amplitude. Two reasons for this phenomenon can be adduced. First, the incoherent backlight decreases the contrast of the interference pattern and photocurrent amplitude as a consequence. Second, the simultaneous infrared illumination redistributes the electrons between different types of local levels, reducing the effective lifetime, nonstationary response of the photoconductivity, and resulting photocurrent.^{16,17}

We have compared two techniques for the drift mobility determination and carried out measurements of the frequency transfer functions of the nonstationary photocurrent excited in ac and dc fields with approximately equal effective values $E_0 \approx 10 \text{ kV/cm}$ (Fig. 9). As follows from this figure the photocurrent generation in an ac field is more efficient in the high-frequency region $\omega > 300 \text{ kHz}$: the signal enhancement with respect to the diffusion regime equals $\sim 70 \text{ dB}$ for the

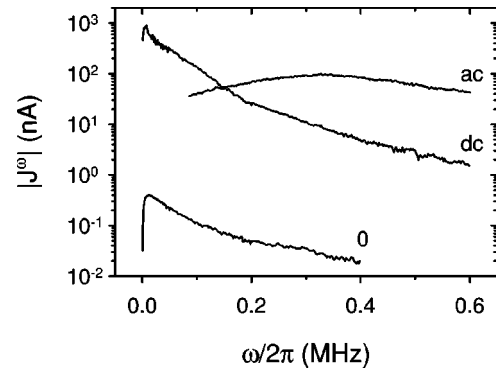


FIG. 9. Frequency transfer functions of the holographic photocurrent measured in ac ($E_0=9.5 \text{ kV/cm}$, $\Omega/2\pi=6 \text{ kHz}$, $T \approx 313 \text{ K}$), dc ($E_0=10 \text{ kV/cm}$, $T=313 \text{ K}$), and zero ($E_0=0$, $T \approx 293 \text{ K}$) external fields. $\lambda=532 \text{ nm}$, $I_0=2.2 \text{ W/cm}^2$, $K=500 \text{ cm}^{-1}$.

case of the ac field and $\sim 50 \text{ dB}$ for the dc one. This fact proves the theoretical estimations [Eqs. (7) and (9)] that predict the prevalence of ac field excitation over the dc one by a factor of $KL_0 \sim 10$.

One can notice the most interesting difference between these two approaches: the frequency transfer function of the nonstationary photocurrent excited in a dc field contains no resonant maximum at high modulation frequencies $\omega > \omega'_0$ [where $\omega'_0/2\pi \approx 20 \text{ kHz}$ is the second cutoff frequency of the nonstationary photocurrent excited without an external field (Fig. 9)].

It is quite difficult to point out the origin of this feature. (i) First the silver paste contacts to $\text{Bi}_{12}\text{SiO}_{20}$ crystals are usually rectifying, so a 10%–20% dc voltage drop in the contact area is expected. This decreases the KL_0 product, partially eliminating the resonant conditions for the dc field. The blocking contact gives rise to the inhomogeneous distribution of the dc field over the interelectrode spacing as well. It makes the resonant frequency dependent on the local value of the electric field, which can result in a blurring of the resonant peak. In the case of the high-frequency ac field ($\Omega > \tau_M^{-1}$) such effects are negligible as the displacement current through the contacts decreases the corresponding voltage drops and makes the electric field more homogeneous.

(ii) Another and perhaps the most essential reason for the discussed difference between photocurrent generation in ac and dc fields can be associated with the complicated processes of conductivity relaxation in $\text{Bi}_{12}\text{SiO}_{20}$. The frequency dependence of the photoconductivity response to the amplitude modulated light¹⁷ is not adequately described by the simplest band transport model with one type of partially compensated donor level. Namely, there are at least two regions where photoconductivity relaxation is characterized by different time constants (Fig. 10). In our experiments the frequency of the ac field ($\Omega/2\pi=6 \text{ kHz}$) was higher than the characteristic frequency separating these regions ($\omega_s/2\pi \sim 100 \text{ Hz}$). We suppose that the frequency transfer functions measured in ac and dc fields differ because the effective photoelectric parameters governing the charge

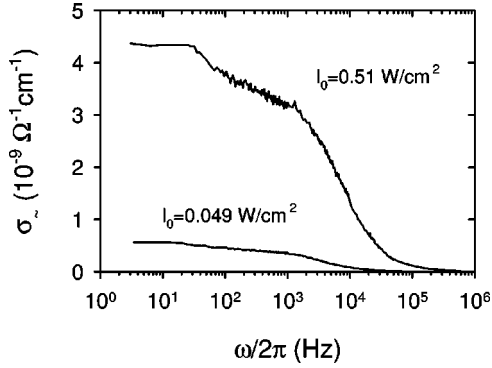


FIG. 10. Frequency dependence of the nonstationary photoconductivity response to the amplitude-modulated light with different average intensities $I_0=0.049, 0.51 \text{ W/cm}^2$. $\lambda=532 \text{ nm}$, $m=0.018$.

transport do not coincide for these cases: $\tau_{ac} < \tau_{dc}$ and $\mu_{ac} > \mu_{dc}$. This assumption is proved by the values of the effective mobility measured by the discussed technique in an ac field, $\mu_{ac}=0.13\text{--}0.8 \text{ cm}^2/\text{V s}$, and the dc one, $\mu_{dc}=0.016\text{--}0.043 \text{ cm}^2/\text{V s}$.^{12,14} So the larger mobility in ac fields helps to fulfill the resonant condition $\omega_r \gg \omega'_0$ and obtain the resonant maximum on the frequency dependence of the photocurrent.

IV. DISCUSSION

The resonant excitation of the nonstationary holographic currents in an ac field has demonstrated several distinctive features that can improve the techniques and devices based on the discussed effect. In particular, the proposed above resonant technique allows direct measurements of the photo-carrier's drift mobility. The utilization of an ac external voltage instead of the dc one minimizes the experimental errors of the mobility measurements since the voltage drop in the contact area is smaller and the electric field distribution in the sample volume is more homogeneous. Besides, variations of the voltage frequency may provide additional possibilities for the characterization of crystals with complicated conductivity relaxation processes.

The drift mobility of electrons in $\text{Bi}_{12}\text{SiO}_{20}$ was measured using this method. It lies in the range $\mu=0.13\text{--}0.8 \text{ cm}^2/\text{V s}$, which is approximately an order lower than the range of the actual mobility, $\mu=3.4\text{--}5.5 \text{ cm}^2/\text{V s}$, estimated by other techniques.^{19,20} On the other hand, the measured values are 3–10 times higher than the ones obtained by the non-steady-state photo-emf method realized in dc fields.^{12,14} So the application of an ac electric field allowed us to partially overcome the difficulties of the mobility measurements in wide-gap semiconductors with shallow energy levels.

The giant signal enhancement in the high-frequency region is another attractive feature of photocurrent generation in an alternating field. The enhancement factor reaches $\sim 70 \text{ dB}$ for low spatial frequencies of the interference pattern against the factor of $\sim 50 \text{ dB}$ typical for the case of dc fields.

For practical applications it is more useful to calculate and compare the signal-to-noise ratio for zero and ac fields. Let us estimate it for the resonant frequency ($\omega = \omega_r \gg \omega'_0$), low spatial frequency ($K^2 L_D^2 \ll 1$), and low load resistance ($R_L \ll Z_{cr}$, where Z_{cr} is the crystal's impedance). For the mentioned frequency region the signal amplitude can be calculated using Eq. (5). The thermal noise of the load resistor is dominant for the diffusion regime of the photocurrent generation: $J_{th} = (4k_B T R_L^{-1} \Delta f)^{1/2}$ (Δf is the detection bandwidth). If the external voltage is applied, then generation-recombination noise can be prevalent: $J_{g/r} = 2e\mu\tau E_0 [S g_0 \Delta f / L (1 + \omega^2 \tau^2)]^{1/2}$ (g_0 is the average generation rate of photoelectrons, and S is the cross section of the illuminated volume).²¹ Finally the magnification of the signal-to-noise ratio equals

$$\frac{(S/N)_{ac}}{(S/N)_0} = \frac{E_0 K^2 L_0^2}{2} \sqrt{\frac{L}{S g_0 k_B T R_L}} \quad \text{for } J_{g/r} \gg J_{th} \quad (10)$$

or

$$\frac{(S/N)_{ac}}{(S/N)_0} = \frac{e E_0 K L_0^2}{2 k_B T} \quad \text{for } J_{g/r} \ll J_{th}. \quad (11)$$

This gain factor is very large: for sensible experimental conditions and crystal parameters ($E_0=10 \text{ kV/cm}$, $K=500 \text{ cm}^{-1}$, $L_0=0.02 \text{ cm}$, $L=0.1 \text{ cm}$, $S=10^{-2} \text{ cm}^2$, $g_0=10^{19} \text{ cm}^{-3} \text{ s}^{-1}$, and $R_L=10^4 \Omega$) it reaches 90 dB. In practice, however, some factors can reduce this striking value: nonlinear recording of the space charge grating, trap saturation, etc.

To summarize we have presented detailed investigations of the nonstationary holographic currents excited in the presence of an external ac electric field. Techniques for the drift mobility determination and signal enhancement are proposed. We believe that the influence of an external ac fields on the photocurrent generation is not restricted to our results. It should be interesting to study photocurrent generation in crystals with other photoelectric parameters (for example, extremely low mobility, conductivity, etc.). A more detailed analysis of the effect is required for semiconductors with a complicated structure of local levels in the forbidden gap.

ACKNOWLEDGMENTS

The authors acknowledge partial financial support from NATO Grant Nos. HTEH.LG 970314 and CNS 972900.

*Electronic address: mb@mail.ioffe.ru

¹M.P. Petrov, S.I. Stepanov, and A.V. Khomenko, *Photorefractive Crystals in Coherent Optical Systems* (Springer-Verlag, Berlin, 1991).

²S.I. Stepanov, V.V. Kulikov, and M.P. Petrov, *Opt. Commun.* **44**, 19 (1982).

³S.I. Stepanov and M.P. Petrov, *Opt. Commun.* **53**, 292 (1985).

⁴Ph. Refregier, L. Solymar, H. Rajbenbach, and J.P. Huignard, *J.*

- Appl. Phys. **58**, 45 (1985).
- ⁵C. Besson, J.M.C. Jonathan, A. Villing, G. Pauliat, and G. Roosen, Opt. Lett. **14**, 1359 (1989).
- ⁶V.A. Kalinin, K. Shcherbin, L. Solymar, J. Takacs, and D.J. Webb, Opt. Lett. **22**, 1852 (1997).
- ⁷M.P. Petrov, V.M. Petrov, V.V. Bryksin, A. Gerwens, S. Wevering, and E. Krätzig, J. Opt. Soc. Am. B **15**, 1880 (1998).
- ⁸P.M. Johansen and H.C. Pedersen, J. Opt. Soc. Am. B **15**, 1366 (1998).
- ⁹G.S. Trofimov and S.I. Stepanov, Fiz. Tverd. Tela (Leningrad) **28**, 2785 (1986) [Sov. Phys. Solid State **28**, 1559 (1986)].
- ¹⁰M.P. Petrov, I.A. Sokolov, S.I. Stepanov, and G.S. Trofimov, J. Appl. Phys. **68**, 2216 (1990).
- ¹¹S.I. Stepanov, I.A. Sokolov, G.S. Trofimov, V.I. Vlad, D. Popa, and I. Apostol, Opt. Lett. **15**, 1239 (1990).
- ¹²I.A. Sokolov and S.I. Stepanov, J. Opt. Soc. Am. B **10**, 1483 (1993).
- ¹³S. Mansurova, S. Stepanov, N. Korneev, and C. Dibon, Opt. Commun. **152**, 207 (1998).
- ¹⁴M.A. Bryushinin and I.A. Sokolov, Phys. Rev. B **63**, 153203 (2001).
- ¹⁵C.-C. Wang, R.A. Linke, D.D. Nolte, M.R. Melloch, and S. Trivedi, Appl. Phys. Lett. **72**, 100 (1998).
- ¹⁶M. Bryushinin, V. Kulikov, and I. Sokolov, Phys. Rev. B **65**, 245204 (2002).
- ¹⁷S.M. Ryvkin, *Photoelectric Effects in Semiconductors* (Consultants Bureau, New York, 1964).
- ¹⁸M.A. Bryushinin, V.V. Kulikov, and I.A. Sokolov, Zhurn. Tekhn. Fiz. (St. Petersburg) **72**, 79 (2002) [Tech. Phys. **47**, 1283 (2002)].
- ¹⁹S.L. Sochava, K. Buse, and E. Krätzig, Phys. Rev. B **51**, 4684 (1995).
- ²⁰I. Biaggio, R.W. Hellwarth, and J.P. Partanen, Phys. Rev. Lett. **78**, 891 (1997).
- ²¹A. van der Ziel, *Noise: Sources, Characterization, Measurement* (Prentice-Hall, Englewood Cliffs, NJ, 1970).